Science
AAAS

Astroglial Metabolic Networks Sustain Hippocampal Synaptic Transmission

Nathalie Rouach, *et al.*

Science **322**, 1551 (2008);
DOI: 10.1126/science.1164022

Astroglial Metabolic Networks Sustain Hippocampal Synaptic Transmission

Nathalie Rouach,[1]* Annette Koulakoff,[1] Veronica Abudara,[1,2] Klaus Willecke,[3] Christian Giaume[1]

Astrocytes provide metabolic substrates to neurons in an activity-dependent manner. However, the molecular mechanisms involved in this function, as well as its role in synaptic transmission, remain unclear. Here, we show that the gap-junction subunit proteins connexin 43 and 30 allow intercellular trafficking of glucose and its metabolites through astroglial networks. This trafficking is regulated by glutamatergic synaptic activity mediated by AMPA receptors. In the absence of extracellular glucose, the delivery of glucose or lactate to astrocytes sustains glutamatergic synaptic transmission and epileptiform activity only when they are connected by gap junctions. These results indicate that astroglial gap junctions provide an activity-dependent intercellular pathway for the delivery of energetic metabolites from blood vessels to distal neurons.

Glucose, transported by the blood, is the major source of energy used by the brain for neuronal activity (*1*). It has been proposed that neurons obtain most of their energy from extracellular lactate, a glucose metabolite produced by astrocytes (*2*). Indeed, astrocytes provide by their perivascular endfeet (*3*, *4*) and processes a physical link between the vasculature and the synaptic terminals, supporting the concept of metabolic coupling between glia and neurons (*2*). Moreover, a typical feature of astrocytes is their network organization resulting from extensive intercellular communication through gap-junction channels formed by connexins (Cxs) (*5*). Thus, the aim of this work was to determine whether and how the connectivity of local perivascular astroglial networks contributes to their metabolic supportive function to neurons.

The expression of Cx43 and Cx30, the main astroglial gap-junction proteins (*6*), is enriched in perivascular endfeet of astrocytes and delineates blood vessel walls in mouse hippocampus (Fig. 1A and fig. S1), as previously described in the cortex for Cx43 (*4*) and Cx30 (*7*). Around blood vessels, Cx immunoreactive puncta are larger than those in the parenchyma and form honeycomb patterns,

[1]INSERM U840, Collège de France, 11 place Marcelin Berthelot, 75005 Paris, France. [2]Facultad de Medicina, Universidad de la Republica, Montevideo, Uruguay. [3]Institute of Genetics, University of Bonn, Roemerstraße 164, 53117 Bonn, Germany.

*To whom correspondence should be addressed. E-mail: nathalie.rouach@college-de-france.fr

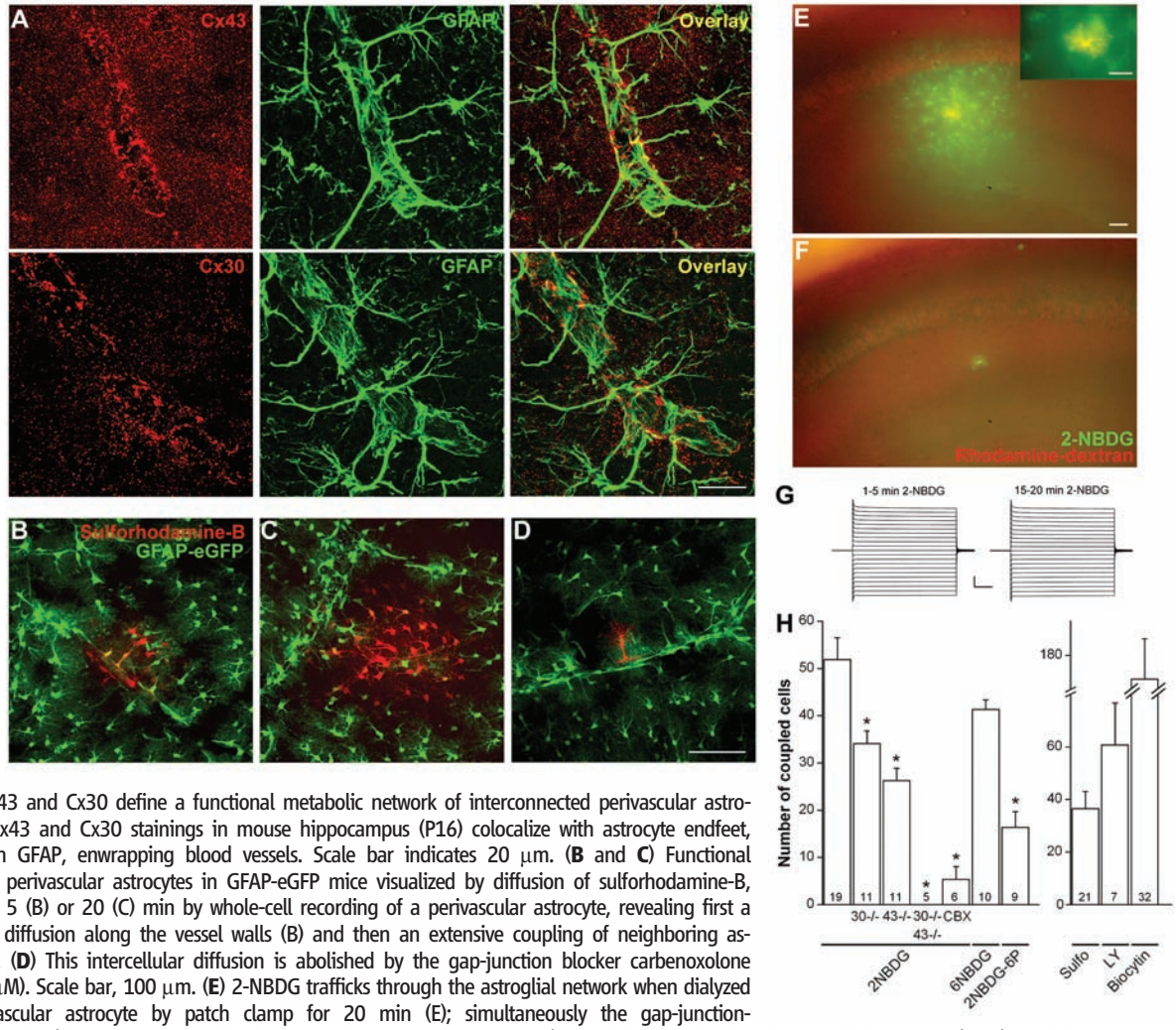

Fig. 1. Cx43 and Cx30 define a functional metabolic network of interconnected perivascular astrocytes. (**A**) Cx43 and Cx30 stainings in mouse hippocampus (P16) colocalize with astrocyte endfeet, labeled with GFAP, enwrapping blood vessels. Scale bar indicates 20 μm. (**B** and **C**) Functional coupling of perivascular astrocytes in GFAP-eGFP mice visualized by diffusion of sulforhodamine-B, dialyzed for 5 (B) or 20 (C) min by whole-cell recording of a perivascular astrocyte, revealing first a preferential diffusion along the vessel walls (B) and then an extensive coupling of neighboring astrocytes (C). (**D**) This intercellular diffusion is abolished by the gap-junction blocker carbenoxolone (CBX, 150 μM). Scale bar, 100 μm. (**E**) 2-NBDG trafficks through the astroglial network when dialyzed in a perivascular astrocyte by patch clamp for 20 min (E); simultaneously the gap-junction-impermeable dye (dextran tetramethylrhodamine, molecular weight = 10,000) was dialyzed to localize the recorded astrocyte (inset). Scale bars, 50 μm. (**F**) 2-NBDG interastrocytic trafficking is mediated by gap junctions because it is abolished by CBX. (**G**) 2-NBDG does not modify within 20 min current/voltage (*I/V*) curve of the recorded astrocyte illustrated in (E). (**H**) Graph summarizing the extent of astrocytic coupling for several fluorescent glucose metabolites (2-NBDG, 6-NBDG, and 2-NBDG-6P) and tracers (Sulfo, sulforhodamine; LY, Lucifer yellow; biocytin) in wild-type and knockout mice for Cxs [30–/–, Cx30–/–; 43–/–, Cx43(fl/fl):GFAP-cre; and 30–/–43–/–, double-knockout Cx30–/–Cx43(fl/fl):GFAP-cre]. Asterisks indicate statistical significance ($P < 0.01$); error bars indicate standard error of mean (SEM).

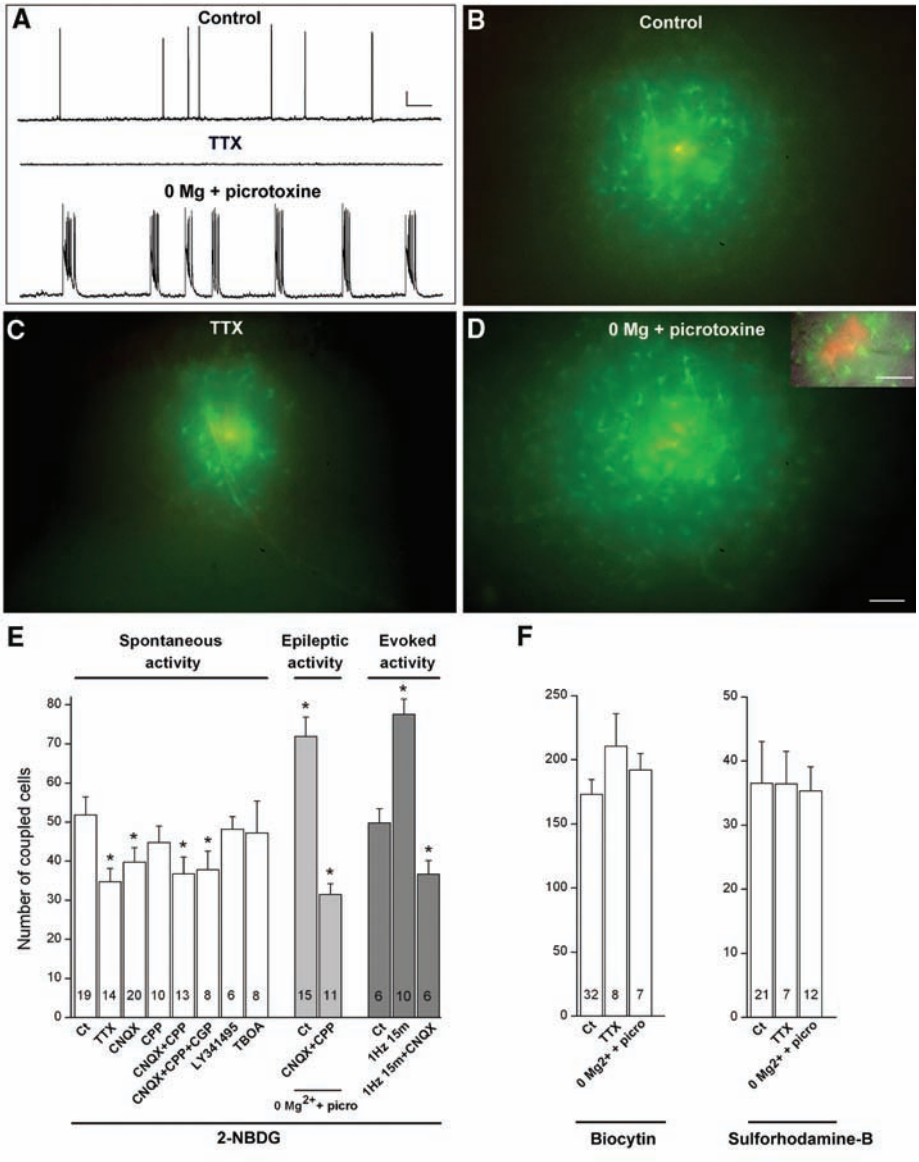

Fig. 2. Activity-dependent glucose trafficking in the astroglia network. (**A**) Spontaneous activity of hippocampal CA1 pyramidal cells recorded in current clamp in control, TTX (0.5 μm, 1 to 4 hours), and 0 Mg^{2+}-picrotoxine (100 μm, 1 to 4 hours) conditions. Scale bar, 20 mV, 6.7 s. (**B** to **D**) Sample pictures showing that 2-NBDG trafficking in astrocytes is decreased in TTX (C) and increased in 0 Mg^{2+}-picrotoxine (D), as compared with control conditions (B). (D Inset) The recorded perivascular astrocyte labeled with dextran tetramethylrhodamine (red) and 2-NBDG (green). Scale bars, 50 μm. (**E**) Graph summarizing the extent of astrocytic coupling for 2-NBDG during spontaneous, epileptic (0 Mg^{2+}-picrotoxine) and evoked activity (1 Hz, 15 min). In all cases, glutamate increases the trafficking of 2-NBDG in astrocytic networks by activating AMPA receptors (AMPARs). All drugs were applied for 1 to 4 hours: CNQX (AMPAR antagonist, 10 μM); 3-(-2-carboxypiperazin-4-yl)-propyl-1-phosphonic acid (CPP) (NMDAR antagonist, 10 μM), (2S)-3-{[(1S)-1-(3,4-Dichlorophenyl)ethyl]amino-2-hydro xypropyl}(phenylmethyl)phosphinic acid (CGP55845) ($GABA_BR$ antagonist, CGP, 2 μM), LY143495 (mGluR antagonist, 20 μM), and threo-b-benzyloxyaspartic acid (TBOA) (glutamate transporter inhibitor, 100 μM). Asterisks indicate statistical significance ($P < 0.01$). (**F**) Biocytin or sulforhodamine-B trafficking in astrocytic networks is not regulated by neuronal activity. Error bars indicate SEM.

outlining the areas of contact between endfeet. Outside blood vessels, Cx43 staining is abundant, whereas Cx30 immunoreactivity is much weaker.

To determine whether gap junctions between perivascular astrocytes are functional, we analyzed the diffusion of gap-junction channel-permeable dyes (sulforhodamine-B, Lucifer yellow) or tracer (biocytin), dialyzed by whole-cell recording of a perivascular astrocyte. A preferential diffusion along the vessel wall was revealed by a 5-min dialysis of sulforhodamine-B (Fig. 1B), whereas a 20-min dialysis resulted in extensive intercellular diffusion into neighboring astrocytes (58 ± 10 cells, $n = 11$) (Fig. 1, C and H). This diffusion was mediated by gap junctions because it was abolished by the gap-junction blocker carbenoxolone (CBX) (Fig. 1D). Most of the coupled cells (133 ± 12 cells for biocytin, $n = 36$) were identified as astrocytes by immunohistochemical staining (fig. S2).

Perivascular astrocytes take up glucose from the blood by the glucose transporter–1 located in their endfeet (*3*). Therefore we investigated whether glucose, once taken up, can traffic through astroglial networks. Glucose trafficking was examined in hippocampal slices by using the fluorescent glucose derivatives 2-[*N*-(7-nitrobenz-2-oxa-1,3-diazol-4-yl)amino]-2-deoxyglucose (2-NBDG) and the nonhydrolyzable 6-[*N*-(7-nitrobenz-2-oxa-1,3-diazol-4-yl)amino]-6-deoxyglucose (6-NBDG) (*8*). When injected for 20 min by whole-cell recordings of astrocytes lining blood vessels in stratum radiatum, 2-NBDG diffused through the astroglial network (52 ± 5 cells, $n = 19$) (Fig. 1E) mediated by Cx30 and Cx43 channels. Indeed, its trafficking was reduced by ~35% in Cx30−/− mice ($n = 11$) and by ~50% in Cx43(fl/fl):glial fibrillary acidic protein (GFAP)–cre mice ($n = 11$) and was totally abolished in the double-knockout mice Cx30−/−Cx43(fl/fl):GFAP-cre ($n = 5$) (Fig. 1H). Interestingly, the trafficking of 2-NBDG-6P, the first phosphorylated metabolite of 2-NBDG, was decreased by ~70% compared with 2-NBDG (Fig. 1H), whereas gap-junction permeability was not affected as indicated by the unchanged cell membrane resistance. This suggests a selectivity of gap-junction channels for energetic metabolites according to their phosphorylation, implying that glucose, rather than glucose-6-phosphate, is a preferred metabolite for gap-junction trafficking. When 2-NBDG was dialyzed into CA1 pyramidal cells and interneurons, it never diffused to neighboring cells (fig. S3, A and D). Moreover, neuronal (fig. S3) and astroglial (Fig. 1G) electrophysiological properties were not altered by the intrapipette 2-NBDG.

Because astrocytes provide energetic substrates to neurons in an activity-dependent manner (*9*), we investigated whether 2-NBDG interastrocytic trafficking was regulated by various regimes of neuronal activity. First, inhibition of spontaneous activity by tetrodotoxin (TTX) (Fig. 2A) decreased 2-NBDG diffusion by ~35% ($n = 14$) (Fig. 2, C and E). In this condition, the basal glutamatergic activity exerts a tonic effect because CNQX reduced by ~25% the number of 2-NBDG–coupled astrocytes (Fig. 2E). In contrast, NMDA (*N*-methyl-D-aspartate), $GABA_B$ (γ-aminobutyric acid type B), metabotropic glutamate receptors, and glutamate transporters were not involved in such regulation (Fig. 2E). Then, intense neuronal activity generated by epileptiform bursts (Fig. 2A) increased by ~40% ($n = 15$) 2-NBDG diffusion in the astroglial network (Fig. 2D), an effect also due to glutamatergic activity because it was abolished by AMPA and NMDA receptor antagonists (Fig. 2E). Lastly, evoked activity by repetitive stimulation of the Schaffer collaterals (1 Hz, 15 min) increased 2-NBDG trafficking in the astroglial network

(+50%, $n = 10$), an effect also mediated by AMPA receptors (Fig. 2E). Therefore glutamate, released by spontaneous, epileptiform, or evoked activity, increases glucose trafficking in astroglial networks by activating AMPA receptors. Because hippocampal astrocytes connected by gap junctions lack AMPA receptors (*10*, *11*), these effects were presumably the consequence of neuronal AMPA receptor activation.

These activity-dependent regulations were specific to glucose. They were not observed when gap-junction-permeable tracers were used (Fig. 2F), suggesting that glutamatergic synaptic activity does not regulate gap-junction channel permeability but may trigger an energetic demand that generates a diffusion gradient for glucose directly linked to the level of neuronal activity. To address this issue, we delivered 2-NBDG in a perivascular astrocyte patched in stratum oriens at an average distance of 30 ± 4 μm ($n = 12$) above the pyramidal cell body layer, whereas a local increase in neuronal demand was induced in stratum radiatum by Schaffer collaterals stimulation (1 Hz, 20 min) (Fig. 3A). Dual extracellular recordings of field excitatory postsynaptic potentials (fEPSPs) revealed that such stimulation evokes a larger glutamatergic synaptic activity in stratum radiatum than in stratum oriens (+392%, $n = 8$) (Fig. 3, B and E), although both recording pipettes were equally distant from the stimulation electrode (279 ± 6 μm versus 264 ± 6 μm, $n = 8$) and from stratum pyramidale (74 ± 5 μm versus 75 ± 5 μm, $n = 8$). In control conditions, 2-NBDG diffusion in astrocytes was largely confined to stratum oriens (75% of the coupled cells, $n = 6$) and occasionally crossed the pyramidal cell body layer to reach stratum radiatum (25% of the coupled cells, $n = 6$) (Fig. 3C). When the Schaffer collaterals were stimulated, the extent of glucose diffusion into stratum pyramidale and radiatum astrocytes almost doubled compared with control conditions ($n = 8$), whereas the number of 2-NBDG positive astrocytes was similar (Fig. 3, D and E). These data suggest that glutamatergic synaptic activity in stratum radiatum signals a local energetic demand that induces the diffusion of 2-NBDG to these sites, resulting in an activity-dependent shape change of astroglial metabolic networks.

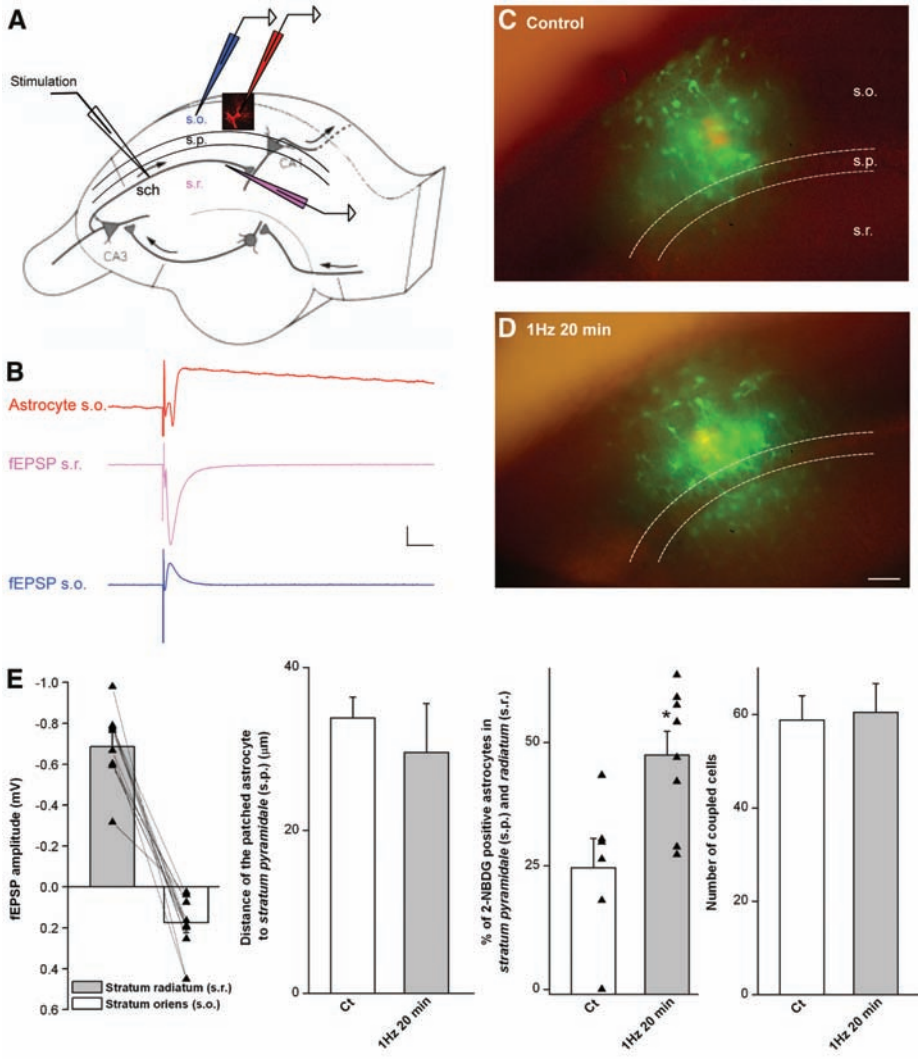

Fig. 3. Activity-dependent change in the shape of astroglial metabolic networks by local energetic demand. (**A**) Schematic drawing depicting recordings of an astrocyte located in stratum oriens (s.o.) at <50 μm from stratum pyramidale (s.p.) with a patch pipette containing both 2-NBDG and tetramethylrhodamine-dextran, during stimulation of the Schaffer collaterals (sch) in stratum radiatum (s.r.). Extracellular pipettes for simultaneous recordings of evoked fEPSPs in s.o. (blue) and s.r. (pink) are also represented. (**B**) Sample traces of the evoked depolarization in s.o. astrocytes (scale bar, 0.5 mV and 12.5 ms) and paired s.o. and s.r. fEPSPs (scale bar, 0.15 mV and 12.5 ms) during stimulation of the sch. (**C** to **E**) Sample pictures and graphs showing that sch stimulation (1 Hz, 20 min, $n = 8$) extends 2-NBDG diffusion to s.r. astrocytes (Ct, control without stimulation, $n = 6$). Scale bar, 50 μm. Error bars indicate SEM.

What might be the role of this glucose trafficking through astroglial networks? To test whether it contributes to glutamatergic synaptic activity, we performed extracellular recordings of fEPSPs evoked by Schaffer collaterals stimulation during exogenous glucose deprivation (EGD), while selectively delivering and increasing intracellular glucose in a single astrocyte via the recording pipette (supporting online text and fig. S4). We hypothesized that glucose can spread into the astroglial network because the number of coupled astrocytes after 1 hour of dialysis with sulforhodamine-B, also included in the patch pipette, reached 87 ± 7 astrocytes ($n = 12$) in wild-type mice (Fig. 4A). To detect local neuroglial interactions involving a group of connected astrocytes, we located the astrocyte recording pipette at 77 ± 5 μm ($n = 19$) from the neuronal extracellular recording pipette. EGD (30 min) induced a slow and reversible depression of synaptic transmission in hippocampal slices (~50%) (Fig. 4, C, E, and G). Such depression of fEPSPs during EGD was not observed when glucose (20 mM) was administered to the astroglial network (Fig. 4, C, E, and G). This effect was suppressed when lactate transport inhibitor α-cyano-4-hydroxycinnamic acid (4-CIN) was applied 10 min before and during EGD (Fig. 4G). This demonstrates that glucose, initially delivered to one astrocyte, is metabolized into lactate, which is then released extracellularly by astrocytes of the metabolic network and taken up by neurons to sustain their synaptic activity. When lactate (20 mM) instead of glucose was provided directly to the astroglial network, the depression of fEPSPs was also inhibited (Fig. 4G). Lactate can thus traffic through astrocytic gap junctions and be used by neurons as an energetic substrate to sustain their excitatory synaptic transmission. When the same experiment was performed in double-knockout mice for Cx43 and Cx30, fEPSPs depression after EGD persisted with a similar kinetic to control conditions, in which intracellular glucose was not provided to the patched astrocyte (Fig. 4, D, F, and G). This suggests that gap-junction-mediated astroglial networks are involved in energetic metabolites trafficking from astrocytes to neurons sustaining their activity and that, in wild-type mice, inhibition of fEPSPs depression by astrocytic glucose is not due to leakage of glucose from the patch pipette. The magnitude and kinetic of fEPSPs depression induced by EGD in control conditions

was similar in wild-type and double-knockout mice for Cx43 and Cx30 (Fig. 4, E and F), suggesting that astroglial glycogen stores and downstream energetic metabolism steps are comparable in both genotypes.

We further investigated the involvement of gap-junction full channels versus Cx hemichannels in providing a pathway for glucose delivery from astrocytes to neurons during EGD. EGD (30 to 60 min) had no effect on astrocytic coupling for sulforhodamine-B (fig. S5, A and B), whereas it slightly decreased (~25%) 2-NBDG coupling (fig. S5, C and D), suggesting again that the activity-dependent regulation of glucose trafficking is selective (Fig. 2). Indeed, EGD (30 to 60 min) decreased glutamatergic synaptic activity by 50 to 80% (fig. S5). Because Cxs also act as hemichannels mediating the release or uptake of molecules in physiopathological conditions (*12*), they could release glucose or lactate, administered to the astrocytic network. However, their involvement was discarded because ethidium bromide uptake by GFAP–enhanced green fluorescent protein (eGFP) astrocytes showed no difference between control and EGD-treated slices (fig. S5, E and F).

Recent work proposed an involvement of astrocytes (*13*) and energetic metabolism (*14*) in epilepsy. Indeed, ketogenic diets and antiglycolytic compounds such as 2-deoxy-D-glucose have antiepileptic properties (*14*). Therefore, we investigated whether glucose from astroglial networks could also sustain epileptiform activity. Epileptiform activity was recorded extracellularly by fEPSPs and consisted of bursts occurring at a frequency of 1.9 ± 0.6 per minute (n = 6) (Fig. 2A). EGD (30 min) almost totally abolished the bursting activity (fig. S6, A and C), whereas intracellular glucose delivery to astroglial networks during EGD maintained 31% of the bursts (fig. S6, B and C). Hence, glucose trafficking through astroglial networks can partially sustain epileptiform activity. This suggests that energy metabolism of astroglial networks may be a promising target for novel antiepileptic drugs.

Our findings identify a previously unknown role for Cx43 and Cx30 gap-junction channels in hippocampal astrocytes. The Cxs constitute the molecular basis for perivascular astroglial metabolic networks, allowing activity-dependent intercellular trafficking of energetic metabolites used to sustain glutamatergic synaptic activity. Importantly, lactate is the final metabolite released by astrocytes and used by neurons to maintain their activity in physiopathological conditions. These data extend the classical model of astroglial energy metabolism in brain function, in which up to now astrocytes were generally considered as single entities. By including gap-junction-mediated metabolic networks of astrocytes, we propose that supply of energetic metabolites involves groups of connected astrocytes to reach more efficiently and distally the sites of high neuronal demand. Gap junctions are directly involved in the metabolic supportive function of astrocytes by providing an activity-dependent intercellular pathway for glucose delivery from blood vessels to distal neurons. Such a pathway may be important to sustain neuronal activity and survival in pathological conditions that alter energy production, such as hypoglycemia or anoxia/ischemia, in which gap-junction channels are still functional (*15*).

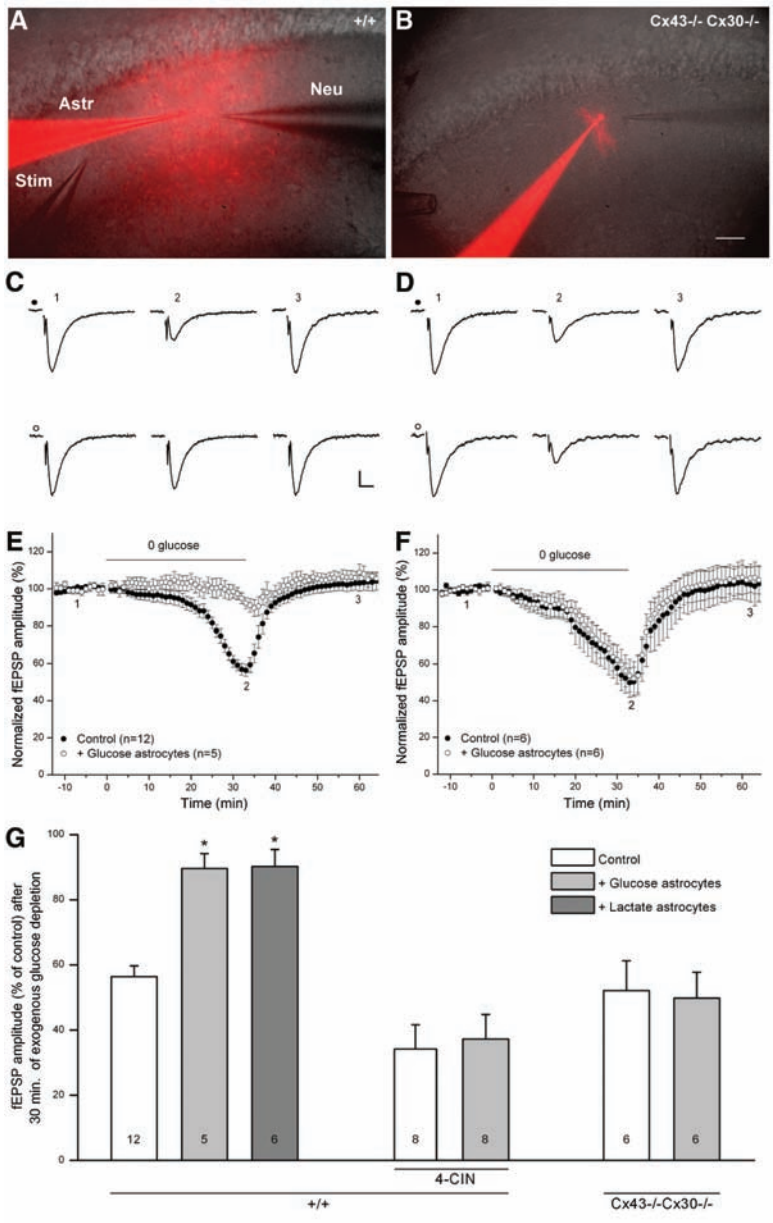

Fig. 4. Metabolic supply through astrocytic networks sustains synaptic transmission during exogenous glucose deprivation. (**A** and **B**) Sample pictures depicting paired recordings of fEPSPs (Neu), evoked by Schaffer collaterals stimulation (Stim), and one astrocyte (Astr) with a pipette containing glucose or lactate (20 mM) and sulforhodamine-B (red, 0.1%). Sulforhodamine-B diffuses extensively in astrocytes from wild-type (+/+) but not from Cx43–/–Cx30–/– mice. Scale bar, 50 μm. (**C** to **G**) Intracellular glucose delivery to astrocytic networks (+ Glucose astrocytes) through the patch pipette inhibits fEPSPs amplitude depression induced by EGD (0 glucose, 32 min) in wild-type [(C) and (E)] but not in Cx43–/–Cx30–/– [(D) and (F)] mice. [(C) and (D)] Sample fEPSPs recorded before (trace 1), during (trace 2), and after EGD (trace 3), as indicated by the numbers in (E) and (F), are shown above the curves. Scale bar, 0.2 mV, 5 ms. (**G**) Graph summarizing fEPSPs amplitude after 30 min of EGD in different conditions [intra-astroglial delivery of glucose (20 mM, + Glucose astrocytes) or lactate (20 mM, + Lactate astrocytes)], lactate transport inhibition by 4-CIN (200 μM) in wild-type (+/+) and Cx43–/–Cx30–/– mice.

References and Notes

1. D. D. Clarke, L. Sokoloff, in *Basic Neurochemistry*, G. J. Siegle, B. W. Agranoff, R. W. Albers, P. B. Molinoff, Eds. (Raven, New York, 1994), pp. 645–680.
2. M. Tsacopoulos, P. J. Magistretti, *J. Neurosci.* **16**, 877 (1996).
3. K. Kacem, P. Lacombe, J. Seylaz, G. Bonvento, *Glia* **23**, 1 (1998).
4. M. Simard, G. Arcuino, T. Takano, Q. S. Liu, M. Nedergaard, *J. Neurosci.* **23**, 9254 (2003).

5. C. Giaume, K. D. McCarthy, *Trends Neurosci.* **19**, 319 (1996).
6. J. I. Nagy, J. E. Rash, *Brain Res. Brain Res. Rev.* **32**, 29 (2000).
7. J. I. Nagy, D. Patel, P. A. Y. Ochalski, G. L. Stelmack, *Neuroscience* **88**, 447 (1999).
8. Materials and methods are available as supporting material on *Science* Online.
9. L. Pellerin, P. Magistretti, *Proc. Natl. Acad. Sci. U.S.A.* **91**, 10625 (1994).
10. K. Matthias *et al.*, *J. Neurosci.* **23**, 1750 (2003).
11. A. Wallraff, B. Odermatt, K. Willecke, C. Steinhauser, *Glia* **48**, 36 (2004).
12. D. C. Spray, Z. C. Ye, B. R. Ransom, *Glia* **54**, 758 (2006).
13. G. F. Tian *et al.*, *Nat. Med.* **11**, 973 (2005).
14. M. Garriga-Canut *et al.*, *Nat. Neurosci.* **9**, 1382 (2006).
15. M. L. Cotrina *et al.*, *J. Neurosci.* **18**, 2520 (1998).
16. We thank P. Ezan for technical assistance and R. Nicoll, G. Bonvento, J. Deitmer, and P. Magistretti for helpful discussions. This work was supported by grants from the Human Frontier Science Program Organization (Career Development Award) and Agence Nationale de la Recherche (Programme Jeunes chercheurs) to N.R.; from INSERM to N.R., A.K., and C.G.; from the German Research Association (SFB 645, B3) to K.W.; and from International Brain Research Organization to V.A. N.R. dedicates this work to her daughter Angela.

Supporting Online Material
www.sciencemag.org/cgi/content/full/322/5907/1551/DC1
Materials and Methods
SOM Text
Figs. S1 to S6
References

31 July 2008; accepted 29 October 2008
10.1126/science.1164022

Activation of Pannexin-1 Hemichannels Augments Aberrant Bursting in the Hippocampus

Roger J. Thompson,[1]*† Michael F. Jackson,[2] Michelle E. Olah,[2] Ravi L. Rungta,[1] Dustin J. Hines,[1] Michael A. Beazely,[2] John F. MacDonald,[2] Brian A. MacVicar[1]†

Pannexin-1 (Px1) is expressed at postsynaptic sites in pyramidal neurons, suggesting that these hemichannels contribute to dendritic signals associated with synaptic function. We found that, in pyramidal neurons, *N*-methyl-D-aspartate receptor (NMDAR) activation induced a secondary prolonged current and dye flux that were blocked with a specific inhibitory peptide against Px1 hemichannels; knockdown of Px1 by RNA interference blocked the current in cultured neurons. Enhancing endogenous NMDAR activation in brain slices by removing external magnesium ions (Mg^{2+}) triggered epileptiform activity, which had decreased spike amplitude and prolonged interburst interval during application of the Px1 hemichannel blocking peptide. We conclude that Px1 hemichannel opening is triggered by NMDAR stimulation and can contribute to epileptiform seizure activity.

Hemichannels are formed by pannexin or connexin proteins and mediate large ionic currents and the passage of small molecules (<1 kD) across plasma membranes. Pannexin-1 (Px1) forms hemichannels in a number of cell types and can be opened by ischemic-like conditions in pyramidal neurons (*1*) or purinergic receptor stimulation in red blood cells (*2*). Px1 has been observed at the postsynaptic density by electron microscopy and colocalization with postsynaptic density protein 95 (PSD95) (*3*); therefore, we hypothesized that Px1 hemichannels may have an undiscovered function at postsynaptic sites. Glutamate mediates excitatory synaptic communication via activation of fast AMPA/kainate and slower *N*-methyl-D-aspartate receptors (NMDARs). We investigated the possibility that NMDAR activation opens Px1 hemichannels because of reports that NMDARs lead to a prolonged but unidentified secondary inward current (*4*–*6*).

Under conditions in which voltage-dependent ion channels were blocked, we recorded NMDAR secondary currents (I_{2nd}) from acutely isolated hippocampal neurons with whole-cell patch clamp and activated them by either repeated (10-s duration at 1-min intervals) (Fig. 1A) or continuous (5 to 15 min) 100 μM NMDA with concomitant voltage commands from –80 to +80 mV (Figs. 1D and 2) (*7*). I_{2nd} was evident as an increase in holding current (Fig. 1A, downward shift in middle trace) and was secondary to the NMDAR because it persisted after washout of the agonist (Fig. 1A). Furthermore, I_{2nd} was blocked by 50 μM carbenoxolone (Cbx) (Fig. 1, A to C), an inhibitor of gap junctions and hemichannels (*8*). We tested a selective small peptide inhibitor of Px1, ^{10}panx (100 μM; WRQAAFVDSY) (*9*, *10*), that blocked I_{2nd} [Fig. 1, B and C; $P < 0.05$, analysis of variance (ANOVA)], whereas a scrambled version, ^{sc}panx (FSVYWAQADR), was ineffective (Fig. 1C; Px1 group, $P > 0.05$, ANOVA). Block of the NMDAR ligand-gated currents with 1 mM kyenurinic acid prevented activation of I_{2nd} (fig. S1). Furthermore, the NMDAR currents were not directly affected by Cbx or ^{10}panx as determined by applying these blockers before activation of I_{2nd} (Fig. 1C; $P > 0.05$, ANOVA). Similar to Px1 activation by ischemia (*1*), I_{2nd} had a linear current-voltage relation (Fig. 1B). Although this differs from some Px1 expression systems (*8*, *9*, *11*), it is similar to the "large-conductance" mode of P2X7 in human embryonic kidney cells (*12*), which may be mediated by Px1 (*9*).

The pores of hemichannels are large enough to permit flux of large molecules (*13*), making dye flux a powerful tool for identifying the involvement of Px1. If Px1 mediates I_{2nd}, then NMDAR activation should evoke efflux of calcein (a non-reactive fluorescent indicator) from hippocampal neurons. We loaded acutely isolated hippocampal neurons with calcein red/orange and with a calcium indicator (Fluo-4 or Fluo-4FF) to monitor activation of the NMDAR. NMDA (100 μM), applied for 5 to 10 min to acutely isolated hippocampal neurons in 0 Mg^{2+} solution to enhance NMDA currents without requiring simultaneous membrane depolarization, evoked rapid rises in intracellular calcium concentration ($[Ca]_i$) that persisted after washout of the agonist. Calcein red/orange efflux from single neurons occurred with a delay (average 7.9 ± 1.6 min; $n = 7$ number of cells) after the NMDA-induced $[Ca]_i$ rise, (Fig. 1, D to F). Dye efflux was blocked when 100 μM ^{10}panx was present (Fig. 1, E and F) (*1*, *14*).

By using RNA interference of Px1 in cultured hippocampal neurons, we next confirmed that the NMDAR-evoked I_{2nd} was due to Px1 hemichannels. We first demonstrated that short hairpin RNA (shRNA) delivered to cultured hippocampal neurons via lentivirus (see supporting online material) reduced Px1 levels. Infection of cultured neurons with green fluorescent protein (GFP) and the shRNA vector was achieved at >80% efficiency and with minimal infection of non-neuronal cells. This resulted in knockdown of the Px1 protein in the total culture to 43 ± 10% of control ($P < 0.05$; ANOVA; $n = 4$), as determined by Western blot analysis with an antibody against a C-terminal region of Px1 (Fig. 2A) (*15*). The remaining 43% may be due to expression of Px1 in other cell types in the culture, such as astrocytes (*16*), and incomplete efficacy of the shRNA. We then used sister cultures to test whether the NMDAR I_{2nd} was reduced after shRNA knockdown of Px1. Intensely GFP-positive (that is, shRNA-expressing) neurons were patch-clamped, and NMDA (100 μM) was applied for 2 to 10 min, which activated I_{2nd} (Fig. 2, B and D). Maximal activation was achieved after 5 min of agonist application (Fig. 2, B and D). The Px1 inhibitor, ^{10}panx (100 μM) blocked activation of I_{2nd} (Fig. 2, C and D), and shRNA-expressing neurons had significantly reduced I_{2nd} (by >70%),

[1]Department of Psychiatry and Brain Research Centre, University of British Columbia, 2211 Wesbrook Mall, Vancouver, BC V6T 2B5, Canada. [2]Robarts Research Institute, University of Western Ontario, London, ON N6A 5K8, Canada.

*Present address: Department of Cell Biology and Anatomy and Hotchkiss Brain Institute, University of Calgary, 3330 Hospital Drive Northwest, Calgary, AB T2N 4N1, Canada.
†To whom correspondence should be addressed. E-mail: rj.thompson@ucalgary.ca (R.J.T.); bmacvicar@brain.ubc.ca (B.A.M.)